Bots Selas TF (Orcid ID: 0000-0003-1844-9247)
Groeneveldt Christianne (Orcid ID: 0000-0003-1742-1517)
Hoeben Rob C. (Orcid ID: 0000-0001-9443-8377)

Preclinical evaluation of the gorilla-derived HAdV-B AdV-lumc007 oncolytic adenovirus 'GoraVir' for the treatment of pancreatic ductal adenocarcinoma

Selas T.F. Bots[1], Tom J. Harryvan[2], Christianne Groeneveldt[3], Priscilla Kinderman[2], Vera Kemp[1], Nadine van Montfoort[2], and Rob C. Hoeben[1]

[1]Department of Cell and Chemical Biology, Leiden University Medical Center, 2333 ZC Leiden, the Netherlands; [2]Department of Gastroenterology and Hepatology, Leiden University Medical Center, 2333 ZA Leiden, the Netherlands; [3]Department of Medical Oncology, Leiden University Medical Center, 2333 ZA Leiden, the Netherlands

Corresponding author: Prof. Rob C. Hoeben, Department of Cell and Chemical Biology, Leiden University Medical Center, Leiden 2333 ZC, the Netherlands. E-mail: r.c.hoeben@lumc.nl

Running title: Preclinical evaluation of oncolytic virus GoraVir

Keywords: pancreatic ductal adenocarcinoma, non-human primate oncolytic adenovirus, tumor-stroma, CD46, xenograft model

Abbreviations: CAF, cancer-associated fibroblast; CAR, coxsackie and adenovirus receptor; EV, empty vector; hAd, human adenovirus; HAdV-C5, human adenovirus type 5; KO, knock-out; nhpAd, non-human primate adenovirus; OVT, oncolytic virotherapy; PDAC, pancreatic ductal adenocarcinoma; TME, tumor microenvironment; WT, wildtype.

This article has been accepted for publication and undergone full peer review but has not been through the copyediting, typesetting, pagination and proofreading process which may lead to differences between this version and the Version of Record. Please cite this article as doi: 10.1002/1878-0261.13561

ABSTRACT

Pancreatic ductal adenocarcinoma (PDAC) is a highly aggressive malignancy which shows unparalleled therapeutic resistance due to its genetic and cellular heterogeneity, dense stromal tissue, and immune-suppressive tumor microenvironment. Oncolytic virotherapy has emerged as a new treatment modality which uses tumor-specific viruses to eliminate cancerous cells. Non-human primate adenoviruses of the human adenovirus B (HAdV-B) species have demonstrated considerable lytic potential in human cancer cells as well as limited preexisting neutralizing immunity in humans. Previously, we have generated a new oncolytic derivative of the gorilla-derived HAdV-B AdV-lumc007 named 'GoraVir'. Here, we show that GoraVir displays oncolytic efficacy in pancreatic cancer cells and pancreatic-cancer-associated fibroblasts. Moreover, it retains its lytic potential in monoculture and co-culture spheroids. In addition, we established the ubiquitously expressed complement receptor CD46 as the main entry receptor for GoraVir. Finally, a single intratumoral dose of GoraVir was shown to delay tumor growth in a BxPC-3 xenograft model at 10 days post-treatment. Collectively, these data demonstrate that the new gorilla-derived oncolytic adenovirus is a potent oncolytic vector candidate that targets both pancreatic cancer cells and tumor-adjacent stroma.

1. INTRODUCTION

Pancreatic ductal adenocarcinoma (PDAC) is a highly aggressive malignancy with a five-year overall survival rate of around 10% (National Cancer Institute). The majority of patients presents with unresectable, locally advanced, or metastatic disease at the time of diagnosis which prohibits curative surgery. Moreover, PDAC shows unrivalled therapeutic resistance due to its genetic and cellular heterogeneity, dense stromal tissue, and immune-suppressive tumor microenvironment (TME) [1]. The promising results of immunotherapies in other types of malignancies led to pre-clinical and clinical studies in PDAC (*e.g.,* checkpoint inhibitors and therapeutic vaccines) both as standalone treatments as well as in combinatorial approaches [2]. Unfortunately, most of these showed only moderate improvements in survival. Hence, there is a need for improved immunotherapies that can overcome the inhibition by the immunosuppressive TME in PDAC [2].

Oncolytic virotherapy (OVT) has emerged as a new anti-cancer treatment and comprises the use of viruses that selectively infect, replicate in, and kill cancerous cells as opposed to healthy cells. Upon virus-induced cell death virus progeny is released, as well as danger- and pattern-associated molecular patterns, and tumor (neo)antigens. Together, these pro-inflammatory molecules can initiate an immune response directed against virus-infected cells as well as against the tumor cells [3]. OVT might be especially powerful to overcome difficulties posed by the genetic and cellular heterogeneity in PDAC as it harnesses a diverse range of anti-tumor activities that could be reactive to a broad range of cancer cells. Human adenoviruses (hAds) are one of the candidate viruses employed in OVT and have shown both efficacy and tolerability in multiple clinical trials [4]. However, clinical outcome was often variable with great patient-to-patient variation [5]. This variability may in part be attributable to varying degrees of preexisting neutralizing immunity directed at circulating hAds types [6, 7]. As a means to circumvent this, non-human primate (nhp) Ads have been considered as an alternative source for the generation of new oncolytic Ad vectors [8]. The nhpAds of the HAdV-B species especially have shown potent and broadly acting oncolytic potential in several tumor types including prostate, bladder, and pancreatic cancer *in vitro* [9]. In addition, no preexisting neutralizing immunity directed against these viruses could be detected in the population.

Therefore, we developed an oncolytic derivative of the gorilla-derived HAdV-B AdV-lumc007 by deletion of one of the Retinoblastoma (Rb)-binding domains in *E1A*. Rb protein is a tumor suppressor and regulates cell cycle progression to S-phase by directly binding to the transcription factor E2F1 [10]. Deletion of this binding domain restricts Ad replication to fast-dividing cells, resulting in tumor-selectivity [11]. This new Ad vector named 'GoraVir' demonstrated superior oncolytic potential compared to human Ad type 5 (HAdV-C5) by virtue of its faster dissemination and increased replication potential cancer cells *in vitro* [9]. However, targeting of cancer cells alone is not sufficient

due to *i.e.* dense stromal tissues that make up the majority of the TME in solid tumors. Additionally, the multilayered barriers of the TME provide a complexity that is not reflected in two-dimensional (2D) culture systems [12, 13]. As such, it remains to be explored whether GoraVir is in fact a suitable candidate for the treatment of PDAC. In this study, we characterized GoraVir's lytic potential in 2D and 3D-culture models of PDAC and established proof-of-concept *in vivo*.

2. MATERIALS AND METHODS

2.1 Cells

Pancreatic cancer cell lines BxPC-3 (RRID:CVCL_0186), PATU-T (RRID:CVCL_1847), and MIA PaCa-2 (RRID:CVCL_0428) were all purchased from the American Type Culture Collection (ATCC, Virginia, USA). Cell lines were authenticated every two years by the Forensic Laboratory for DNA Research, Department of Human Genetics, Leiden University Medical Centre, by short tandem repeat analyses and comparison with the STR databases. The patient-derived human pancreatic cancer cell line FNA005 was obtained in December 2019 at the Leiden University Medical Center from a single fine-needle biopsy [14] conform the standards set by the Declaration of Helsinki and cultured in RPMI-1640 (Biowest, Nuaillé, France) supplemented with 8% fetal bovine serum (FBS, Invitrogen, California, USA) and 1% Penicillin-Streptomycin (P/S, Gibco, Massachusetts, USA). Tumor identity was established using AmpliSeq Cancer Hotspot Gene Panel V2 genome sequencing (Thermo Fisher Scientific, Massachusetts, USA). Use of the material was undertaken with the understanding and written consent of the subject and approved by the Medical-Ethical Review Committee (MTCC) Leiden Den Haag Delft (LDD) under issuance protocol no. B21.073. The pancreatic stellate cell line PS-1 was kindly provided by prof. Kocher (Queen Mary University London, London, UK) and has been described previously [15]. Primary pancreatic cancer-associated fibroblasts (CAFs) were isolated as described previously [16] and cultured in Dulbecco's Modified Eagle's Medium (DMEM)/F-12 (Gibco) supplemented with 8% FBS and 1% P/S. Cells were cultured in DMEM supplemented with 8% FBS and 1% P/S unless stated otherwise. All cell lines were confirmed negative for mycoplasma contamination.

2.2 Adenoviruses

All experiments were performed using CsCl-purified Ad stocks. A detailed outline of the CsCl-purification method for Ads has previously been described [9]. GoraVir is a replication-competent vector derived from the HAdV-B gorilla AdV-lumc007 that carries a small deletion in one of the Rb-binding domains of *E1A* and has been described elsewhere [9]. HAdV-C5Δ24E3 is a replication-

competent E3-deleted vector that carries a similar deletion in one of the Rb-binding domains of *E1A* and has also been previously described [11].

2.2 Cell killing assay

For monolayer infection, cells were seeded at 1 x 10^4 cells per well in a flat bottom 96-well plate in normal cell culture medium and incubated o/n at an atmosphere of 5% CO2 at 37°C. For the generation of monoculture spheroids, cells were seeded at 1 x 10^4 cells per well in a 96-well U-bottom plate (Corning Costar, New York, USA) in culture medium supplemented with 0.25% methylcellulose (Sigma-Aldrich, Missouri, USA) and centrifuged at 300 x g for 1 min. Cells were cultured at an atmosphere of 5% CO2 at 37°C for two days to allow for the formation of spheroids. On the day of infection, supernatant was removed and cells were infected at the indicated multiplicity of infection (MOI) in culture medium supplemented with 2% FBS and 1% P/S. Cell viability was measured after 5-6 days using the cell proliferation reagent kit WST-1 (Merck, New Jersey, USA) according to manufacturer's instructions.

2.4 IHC of spheroid co-cultures

BxPC-3 and PS-1 cells were co-cultured using 2.5 x 10^5 cells per well of each cell line in a 96-well U-bottom plate (Corning Costar) in culture medium supplemented with 0.25% methylcellulose and centrifuged at 300 x g for 1 min. Cells were incubated at an atmosphere of 5% CO2 at 37°C for two days to allow for the formation of spheroids. Next, spheroids were collected in 15 mL tubes using a P1000 pipet. When all spheroids had drifted to the bottom of the tube, supernatant was discarded and replaced by 500 µl virus at MOI 10 in cell culture medium supplemented with 2% FBS and 1% P/S. Spheroids were plated in an ultra-low attachment 24-well flat bottom plate (Corning Costar) using 10-20 spheroids per well. After 5 days, spheroids were collected and paraffin-embedded sections were used in IHC using anti-adenovirus hexon antibody (1:2000) and biotinylated goat-α-mouse secondary antibody (1:200, #E0433, Agilent technologies, California, USA). Immunoreactivity was visualized using VECTASTAIN® Elite ABC-HRP kit (Vector Laboratories, California, USA) and DAB substrate (DAKO, Denmark) according to manufacturer's instructions. Counterstain was performed using hematoxylin (Sigma-Aldrich). Light microscopy pictures were obtained using an Olympus BX51 (Olympus Scientific Solutions, Tokyo, Japan).

2.5 Generation of CD46-KO cell lines

Single guide RNAs (sgRNAs) were designed against human CD46 (forward: 5'-CACCGAAGGAAAGGGACACTCGCGG-3'; reverse: 5'-aaacCCGCGAGTGTCCCTTTCCTTC-3') and cloned in a BsmBI-digested plentiCRISPRv2-puromycin vector (#98290, Addgene, Cambridge, UK) as described elsewhere [17]. Sanger sequencing was performed to verify the correct insert of the sgRNA using an

U6-promoter primer (forward: 5'-GAGGGCCTATTTCCCATGATT-3'). For the generation of an empty vector (EV) control cell line, a BsmBI-digested plentiCRISPRv2-puromycin vector was used in which no sgRNA was cloned. Subsequently, lentiviruses were generated using third-generation packaging vectors and HEK293T cells according to standard techniques [18]. One day prior to infection 4 x 10^5 cells of A549 or MIA PaCa-2 were seeded per well in a 6-well plate (Thermo Fisher Scientific) in normal cell culture medium. Next, 500 µL virus-containing supernatant was mixed with 500 µL cell culture medium supplemented with 20 µg/mL polybrene (Merck). Cells were transduced for 48 hours and transferred to a T-25 flask (Greiner Bio-one, Kremsmünster, Austria) and puromycin selection (2 µg/mL, Sigma-Aldrich) was performed. From the surviving cells which were transduced with the vector containing sgRNAs against CD46, pure CD46-negative populations were isolated by fluorescence-activated cell sorting (FACS) using a BD FACSAria II 3L (BD). Isolated populations were subsequently cultured in cell culture medium supplemented with puromycin and an atmosphere of 5% CO2 at 37°C. EV control cells were not sorted and cultured under similar conditions.

2.6 Flow Cytometry

Cells were stained extracellular with primary antibodies anti-CAR (1:1000, #05-644, Milipore, Millipore, Massachusetts, USA), anti-CD46 (1:125, #555948, BD), or DSG-2 PE (1:150, #12-9159-42, Invitrogen) according to standardized methods. For intracellular staining, cells were fixed using 4% paraformaldehyde at 4°C for 20 min and permeabilized using Cytofix/Cytoperm™ (BD, New Jersey, USA) before staining with anti-adenovirus hexon (1:1000, #ab8251, Abcam, Cambridge, UK). As a secondary antibody goat-α-mouse PE (1:1000, #12-4010-82, eBioscience) was used. Samples were analyzed using a LSR-II cytometer (BD) and analyzed using FlowJo software (version 10.8.0).

2.7 Animal experiments

Mouse experiments were permitted by the animal welfare body (IvD) of Leiden University Medical Center and carried out under the project license AVD1160020187004 issued by the national competent authority on animal experiments (CCD), in accordance with the Dutch Act on Animal Experimentation and EU Directive 210/63/EU. Male and female nonobese diabetic (NOD).Cg-Prkdc^{scid}Il2rg^{tm1Wjl}/SzJ (NSG) mice (RRID:IMSR_JAX:005557) were obtained from The Jackson Laboratory and maintained at the breeding facility of the LUMC in Leiden, The Netherlands. Mice were 12 weeks old at the start of the experiment and were housed in individually ventilated cages with no more than 4 mice/cage. For tumor challenge, low-passage BxPC-3 cells were harvested and 5 × 10^6 cells in 100 µl PBS supplemented with 0.1% BSA were implanted subcutaneously. Mice body weight was monitored throughout the experiment. Tumor volume was measured three times a week using a caliper and calculated (tumor volume = width × length × height). When all tumors reached a size of

50–200 mm^3 mice were distributed equally among the three treatment groups (n=5/group) according to tumor size and gender and groups were randomly assigned to a particular treatment. Tumors were treated with PBS, GoraVir, or HAdV-C5Δ24E3 by intratumoral injection of 1×10^8 plaque-forming units (pfu) virus in 30 µl PBS under isoflurane anesthesia. Treatment was not blinded. Ten days after treatment, mice were sacrificed by CO_2 inhalation and tumor, spleen, liver, and serum were collected for real-time (RT) quantitative (q)PCR analyses.

2.8 Adenovirus genome copies

Genomic DNA was isolated using the Purelink™ Genomic DNA Kit (K182000, Invitrogen) according to the manufacturer's instructions and DNA concentrations were determined by NanoDrop™ 1000 Spectrophotometer (Thermo Fisher Scientific). Adenovirus genome copies were determined as described previously [9].

2.9 Statistical analyses

All statistical analyses were performed using GraphPad Prism software (v9.0.1, La Jolla, CA). Data are presented as mean ± SEM unless otherwise stated. Unpaired analyses (one-way ANOVA and unpaired t tests) were used for analysis of repeated experiments, and $p < 0.05$ was considered significant throughout. Detailed descriptions about statistical analysis are described in the figure legends. Significant differences are indicated by asterisks, with p values < 0.05 shown as *, <0.01 as **, and <0.001 as ***.

3. RESULTS

3.1 GoraVir shows strong lytic potential in cancer cells and cancer-associated fibroblasts *in vitro*

GoraVir is an oncolytic derivative of the HAdV-B AdV-lumc007 isolated from a gorilla and demonstrated strong oncolytic potential at high MOI in an *in vitro* screening panel consisting of 29 tumor cell lines encompassing four tumor types including glioblastoma, bladder cancer, prostate cancer, and pancreatic cancer [9]. To validate GoraVir's ability to kill pancreatic cancer cells, BxPC-3, PATU-T, MIA PaCa-2, and a low-passage patient-derived pancreatic cancer cell line (FNA005) were infected at MOI 0.1 and 10 with GoraVir or HAdV-C5, as a reference control (Figure 1A). Infection with GoraVir at both MOI resulted in (near-)complete cell killing in all four cell lines at 6 days post infection, except for MIA PaCa-2 at MOI 0.1 (mean residual viability 94,0 ± 1,52 %). Infection with HAdV-C5 also resulted in strong cell killing at MOI 10 in all cell lines although slightly less effective than GoraVir. In line with this, infection with HAdV-C5 at low MOI resulted only in moderate cell killing. Similar observations were made when calculating the EC50 values for both viruses in these cell lines

(Supplementary Table S1). These data validated our previous observations that GoraVir demonstrated superior cytotoxicity in pancreatic cancer cells compared to HAdV-C5.

In PDAC, cancer-associated fibroblasts (CAFs) are a highly abundant cell population and linked to the establishment of an immunosuppressive TME [19]. Consequently, therapeutic strategies targeting these cells have gradually emerged [20, 21]. Recently, it was demonstrated that oncolytic mammalian orthoreovirus (reovirus) was able to infect and kill human untransformed CAFs isolated from several gastrointestinal tumor types *in vitro*, in contrast to an oncolytic derivative of HAdV-C5 [16]. To investigate whether GoraVir does have the potential to infect and lyse CAFs, the pancreatic stellate cell line PS-1 was exposed to GoraVir or HAdV-C5 at high and low MOI and cell viability was determined at 6 days post infection (Figure 1B). Similar to pancreatic cancer cells, GoraVir induced near-complete cell killing in PS-1 at MOI 10 and retained a strong lytic potential at a lower MOI. In contrast, HAdV-C5 showed minor cytotoxicity at MOI 10 (mean residual viability 80,6 ± 3,58 %) and no cell killing at a lower MOI. To continue our exploration of GoraVir's ability to infect and kill CAFs, we exposed patient-derived primary fibroblasts previously isolated from pancreatic cancer tissues [16] with GoraVir at MOI 10 and measured cell viability at 5 days post infection. Again, GoraVir was shown to induce cell killing in the majority of primary fibroblasts (Figure 1C). In fact, for 8 out of 13 fibroblast cell lines cell viability was reduced by ~ 50% or more. Taken together, it appears that GoraVir demonstrates strong lytic potential in pancreatic cancer cells as well as tumor-associated stromal cells.

3.2 GoraVir productively infects and lyses 3D tumor spheroids and tumor-fibroblast co-cultures of PDAC

Spheroid cultures of PDAC are an interesting model for *in vitro* drug testing as they resemble more closely the *in vivo* setting by mimicking important pathobiological aspects, including cell-cell and cell-matrix interactions [13]. To validate whether GoraVir demonstrates its oncolytic potential in 3D models, we first generated monoculture spheroids of BxPC-3 or FNA005 cells (Figure 2A). Spheroids were infected with GoraVir or HAdV-C5 at different MOI and cell viability was measured at 5 days post infection. In the BxPC-3 spheroids, infection with GoraVir showed a considerable reduction in cell viability at MOI ≥ 30 (mean residual viability 43.5 ± 19.3%) although this did not increase upon higher MOI (Figure 2B). In contrast, infection with HAdV-C5 did not result in any cell killing at any MOI tested. Infection of the FNA005 spheroids showed a similar trend, where GoraVir-infected spheroids demonstrated a dose-dependent reduction in cell viability ultimately nearing complete cell killing at MOI 100 (mean residual viability 7.83 ± 6.8%) while cell viability of HAdV-C5-infected spheroids did

not decrease (Figure 2C). In conclusion, GoraVir demonstrated to be significantly more potent in killing monoculture tumor spheroids, similar to what was observed in monolayer cultures.

The inability of HAdV-C5 to kill spheroid monocultures of the two cell lines could be related to a higher resistance to infection at baseline, as illustrated by the infection of monolayer cell cultures in Figure 1. Therefore, we sought to determine whether GoraVir's superior oncolytic potential was attributable to a higher infection efficiency. Tumor-fibroblast spheroids were generated, consisting of cancer cells and PS-1 cells, since cancer cells alone did not allow for the formation of spheroids suitable for immunohistochemistry analyses. Similarly, the FNA005-fibroblast spheroids were shown to disintegrate upon processing and were excluded from subsequent experiments (Figure 2A). BxPC-3-fibroblast spheroids were infected with GoraVir or HAdV-C5 at MOI 10 and stained for Ad hexon protein at 3 days post infection (Figure 2D). Infection with GoraVir resulted in a clear penetration of the tumor-fibroblast spheroids by the virus, illustrated by a considerable number of hexon-positive cells. Moreover, some cells showed a cytopathic phenotype (indicated by the black arrows). Conversely, infection with HAdV-C5 did not yield any hexon protein in the co-culture spheroids at 3 days post infection, similar to the uninfected control. Nevertheless, hexon staining was observed at 5 days post infection with HAdV-C5. As such, it appears that HAdV-C5 can infect co-culture spheroids albeit less efficiently than GoraVir. In support of this, very few GoraVir-infected spheroids could be retrieved at day 5 post infection. The absence of intact spheroids is most likely due to the loss of integrity caused by the combined effect of the infection as well as the formation of a necrotic core after longer periods of culturing [22]. Taken together, it appears that GoraVir lytic potential in 3D culture models of PDAC can be attributed to its ability to efficiently infect and penetrate tumor spheroid cultures.

3.3 GoraVir uses CD46 as its primary entry receptor into human cells

The superior cytolytic efficacy of GoraVir, compared to HAdV-C5, and its broad tropism prompted us to explore the mode of entry of this virus. For entry into the host cell, Ads bind their primary receptor via the fiber knob, followed by secondary interactions between the penton-base proteins and integrins on the cell surface, leading to endocytosis of the virion into the host cell [23]. Ads of the HAdV-C species make use of the coxsackie and adenovirus receptor (CAR) for entry into the host cell [24, 25]. Reduced expression of CAR has shown to be a major limiting factor in transduction efficiency and elaborate efforts have been made to retarget these vectors by e.g., replacement of the fiber knob protein [26–29]. Most hAds, as well as several chimpanzee-derived Ads, of the HAdV-B species make use of cluster of differentiation 46 (CD46) protein as their main entry receptor into human cells 30,

31]. CD46 is a membrane protein involved in the regulation of complement deposition, ubiquitously expressed on nucleated cells, and its expression is upregulated in many tumor types [32]. Considering GoraVir's broadly acting oncolytic potential and genomic resemblance to members of the HAdV-B species [9], we hypothesized that it uses this receptor for viral entry into the host cell. Interestingly, we observed a ~50 to 500-fold higher CD46 expression mRNA expression than CAR mRNA expression levels in the patient-derived primary fibroblasts (Supplementary Figure S1). Therefore, CD46 might pose a valuable receptor for targeting of cancer cells as well as CAFs in PDAC.

To determine whether GoraVir indeed makes use of CD46 for entry into human cells, a stable CRISPR/Cas9-mediated CD46-knockout cell line was established in MIA PaCa-2 and A549 cells. After FACS sorting the CD46-negative population (CD46-KO), cells were checked for the expression of the three receptors frequently used by hAds for viral entry: CAR, CD46, and desmoglein-2 (DSG-2) [30]. Wildtype (WT) and empty vector (EV) control cells for both cell lines showed high surface expression of CD46 and DSG-2, and to a lesser extent, CAR (Figure 3A; Supplementary Figure S2A). While surface expression of CAR and DSG-2 was maintained in the two CD46-KO cell lines, no CD46 expression could be detected, thereby confirming the CRISPR/Cas9-mediated knockout of CD46 (Figure 3A, Supplementary Figure S2A). Next, cells were infected with GoraVir or HAdV-C5 and hexon protein expression was measured at 24 or 48 hours post infection for A549 cells (Supplementary Figure S2B) and MIA PaCa-2 (Figure 3B), respectively. Compared to WT and EV cells, deletion of CD46 strongly reduced the number of hexon-positive cells upon infection with GoraVir but not HAdV-C5, in both MiaPaCa2 and A549 cells. In fact, infection of the MIA PaCA-2 CD46-KO cells with GoraVir was similar to uninfected cells (Figure 3C), suggesting the virus was no longer able to enter the cells. For A549 cells, a less prominent but significant reduction was observed in the absence of CD46 compared to WT ($p=0.015$) and EV cells ($p=0.012$) (Supplementary Figure S2C). One explanation why GoraVir was still able to enter A549 CD46-KO cells might be due to the use of an alternative route of entry in these cells, as has been observed for fiber gene-deleted HAdV-C5 vectors [34].

To confirm that the inability to enter cells directly influenced its ability to kill these cells, all cell lines were infected with GoraVir or HAdV-C5 at different MOI and cell viability was measured at 6 days post infection. As expected, the MIA PaCa-2 CD46-KO cell line showed no killing upon infection with GoraVir at any of the MOI tested (Figure 3D). In contrast, the absence of CD46 had no inhibitory effect on cell killing with HAdV-C5 (Figure 3E). Similar observations were made in the A549 CD46-KO cell line at 3 days post infection although the phenotype after infection with GoraVir was lost upon higher MOI (Supplementary Figure S2D-E). These observations are in line with the relatively high amount of virus still being able to enter the cells at MOI 10 (Supplementary Figure S2B). Nevertheless, it seems that the absence of CD46 strongly reduces GoraVir's ability to infect and kill these cancer cell lines.

Moreover, the observation that infectivity was similar to uninfected cells in the MIA PaCa-2 cell line strongly suggests that CD46 can be used as a (primary) entry receptor by GoraVir.

3.4 A single intratumoral dose of GoraVir delays tumor growth in a xenograft NGS mouse model

To continue our preclinical evaluation of GoraVir *in vivo*, we used a BxPC-3 xenograft model and tested the virus in parallel with an oncolytic derivative of HAdV-C5 (HAdV-C5Δ24E3) which harbors a similar deletion in the Rb-binding domain of *E1A* as to increase its tumor selectivity [35]. Prior to the experiment, no differences in lytic potential were observed between HAdV-C5 and HAdV-C5Δ24E3 in the BxPC-3 cell line *in vitro* (data not shown). NSG mice were subcutaneously injected with BxPC-3 cells and palpable tumors were treated intratumorally with a single dose of 1 x 10^8 pfu virus, or PBS as a control. Tumor growth was monitored and animals were sacrificed on day 10 post treatment for further analyses. All treatments were well-tolerated by the animals throughout the experiment (Supplementary Figure S3). In the first days after treatment with either GoraVir or HAdV-C5Δ24E3, but not the PBS control group, a small reduction in tumor growth was observed for several mice (Figure 4A). However, all tumors grew out exponentially thereafter. Although exponential outgrowth was observed in all groups, there seemed to be a delay in tumor growth in the GoraVir-treated mice compared to HAdV-C5Δ24-treated mice or the PBS control group. Indeed, pooled analysis of the three treatments groups revealed a significant reduction in mean tumor volume in the GoraVir-treated group (548.8 ± 53.7 mm^3) compared to the PBS control group (781.6 ± 147.8 mm^3, p=0.010) and HAdV-C5Δ24E3-treated group (883.2± 83.4 mm^3, p<0.001) at day 10 post treatment (Figure 4B). Interestingly, tumor volume of HAdV-C5Δ24-treated tumors was somewhat increased compared to PBS-treated tumors although this was not statistically significant. Measurements of tumor weight followed a similar trend with a reduction in mean tumor weight in the GoraVir-treated group (0.380 ± 0.061 g) compared to the PBS control group (0.441 ± 0.064 mm^3, p=0.200) and HAdV-C5Δ24E3-treated group (0.541 ± 0.024 mm^3, p=0.001). Interestingly, tumor weight of HAdV-C5Δ24E3-treated tumors was significantly increased compared to PBS-treated tumors (p=0.028).

To determine whether the observed reduction in tumor volume and tumor weight in GoraVir-treated mice compared to HAdV-C5Δ24E3-treated mice was associated with a difference in viral replication, the number of viral genomes were determined in the tumor tissues. PBS-treated tissues were used as a baseline. Interestingly, no differences in viral genome copies were found in tumors of GoraVir and HAdV-C5Δ24E3-treated mice (Figure 3D). Likewise, similar levels were observed in other sites inherent to Ad biodistribution in mice including serum, liver, and spleen, collected at the time of sacrifice 29, 36]. Note, however, that in 1/3 serum samples of HAdV-C5Δ24E3-treated mice no Ad DNA could be

detected (two samples did not yield enough DNA for RT-qPCR analysis) as well as 1/5 samples of GoraVir-treated mice. Taken together, it seems that the observed delay in tumor growth upon administration of a single intratumoral dose of GoraVir might not be attributable to increased viral replication compared to HAdV-C5Δ24E3. Therefore, it remains to be established which viral (or cellular) mechanisms underlie the observed differences between the two viruses and enable GoraVir to maintain lytic potential *in vivo*.

4. DISCUSSION

Oncolytic viruses demonstrate to constitute a new treatment approach which has the potential to transform the inaccessible, immunosuppressive TME that is characteristic of PDAC. Here, we studied the oncolytic potential of GoraVir, a new gorilla-derived oncolytic Ad, in various *in vitro* model systems of PDAC and established proof-of-concept of oncolysis *in vivo*. In 2D cell cultures, GoraVir showed strong lytic potential in both cancer cells as well as CAFs (Figure 1). Moreover, GoraVir retained its lytic potential in 3D spheroid culture systems of PDAC in contrast to HAdV-C5 (Figure 2). Dual targeting of tumor as well as stromal compartments improves virus replication and spread and has shown to promote antitumor activity [37, 38]. However, few oncolytic viruses demonstrate natural stroma targeting. This has resulted in the generation of several genetically modified or bioselected variants with enhanced targeting to these compartments [38]. To our knowledge, this is the first report of an oncolytic adenovirus that naturally targets human primary pancreatic CAFs. Previously, the oncolytic adenovirus ICOVIR15 was shown to infect and kill fibroblast activation protein $(FAP)^+$ fibroblasts in a murine glioblastoma model [39]. Another approach to target CAFs using ICOVIR15 included the incorporation of a bispecific T-cell engager directed at FAP [40]. Meanwhile, a recent paper by Harryvan et al. showed that the more wildtype-like HAdV-C5Δ24 was unable to induce cell death in human primary CAFs in contrast to wildtype and bioselected mutant reoviruses [16]. Since the resistance to Ad infection was also observed in CAR-expressing fibroblasts, the authors attributed these differences to the Δ24-modification in the HAdV-C5Δ24 vector, which makes it not suitable for infecting and killing of quiescent cells with an intact Rb-pathway. However, GoraVir harbors a similar deletion in *E1A* and demonstrated considerable potential to kill primary fibroblasts (Figure 1B). This could indicate that CAFs do support productive infection of Rb-dependent oncolytic Ads. Furthermore, the observation that patient-derived primary fibroblasts express higher levels of CD46 mRNA than CAR mRNA led us to speculate the use of a differential receptor, or the expression levels thereof, influences the ability of these viruses to kill CAFs. Future studies examining the ability of the various Ad types to infect CAFs might provide insight in the mechanisms that underly the differences in lytic potential of these Ads in the CAFs.

As anticipated, GoraVir was shown to make use of CD46 for entry into the host cell (Figure 3). CD46 is a membrane protein involved in regulation of the complement and is frequently upregulated in cancer cells to primarily evade antibody-mediated cytotoxicity [41]. The ubiquitous expression of this receptor and its increased expression in many tumors would make it a preferred natural entry receptor of oncolytic Ads [32]. Interestingly, retargeting of HAdV-C5 to CD46 has previously demonstrated to enhance anti-tumor efficacy compared to wildtype virus despite comparable protein expression of CAR and CD46 in the tumor [42, 43]. Taken from this, it appears that targeting of CD46 brings additional benefits despite its ubiquitous expression on cells. CD46 has not been demonstrated to play a direct role in cell death although intracellular complement activation can regulate cell survival via metabolic processes (reviewed in [41, 44]). Alternatively, in bladder cancer cells, retargeting of adenovirus to CD46 was associated with increased transduction efficacy and subsequent cytotoxicity [42]. Hence, the use of CD46 might simply result in faster viral entry which provides these viruses with a head start. Nevertheless, it remains to be established whether the differences between GoraVir and HAdV-C5 are indeed (partially) receptor-dependent.

Finally, we addressed whether the superior cytotoxicity of GoraVir *in vitro* also translated to increased oncolytic activity *in vivo*. In these experiments we opted for intratumoral injection instead of intravenous delivery as this provides a fair comparison of GoraVir and HAdV-C5Δ24E3 given the markedly distinct expression patterns of CAR and CD46 in mice. A single-dose intratumoral injection of GoraVir indeed delayed tumor growth compared to PBS-treated and HAdV-C5Δ24E3-treated mice (Figure 4). The significant reduction in tumor volume at 10 days post treatment seems promising, as anti-tumor effects of oncolytic viruses in pancreatic xenograft models have frequently been observed at later time points [45, 46]. Moreover, a similar dose of HAdV-C5Δ24E3 did not show any anti-tumor activity in our model. Interestingly, no differences in viral genome copies were found in tumor, serum, liver, and spleen between the two viruses upon sacrifice. A possible explanation for the absent correlation between viral replication and anti-tumor activity could be that murine CAR can function as a receptor for hAds, unlike murine CD46, thereby increasing the relative amount of (non-cancerous) cells that might support limited replication of HAdV-C5 [47]. Alternatively, deletion of the entire E3 gene region in HAdV-C5Δ24E3 might have crippled the virus' lytic potential due to the loss of the adenovirus death protein (ADP) [48]. It should be noted that the use of an immunodeficient mouse model to assess anti-tumor efficacy in this study does not accurately address the interplay of the oncolytic virus with the host immune system. Importantly, this interplay is considered a major determining factor for the anti-tumor efficacy of oncolytic viruses. In support of this, oncolytic virus monotherapy frequently generates modest results in patients while combination therapies using other immunotherapies were demonstrated to be much more effective [49]. Consequently, the anti-

tumor effects of GoraVir demonstrated here are likely an underestimation of its true potential. However, strong lytic potential does not always confer the induction of adequate anti-tumor immune responses and may greatly vary between different OVs [50]. Therefore, it would be of interest to determine whether GoraVir induces cancer cell death that that will mediate such anti-tumor immune responses.

5. CONCLUSION

In conclusion, we have shown that GoraVir has strong lytic potential in pancreatic cancer cells and pancreatic CAFs and that this is facilitated by its use of CD46 for viral entry. Moreover, GoraVir demonstrated superior oncolytic efficacy in spheroid culture models of pancreatic cancer and displayed enhanced anti-tumor activity *in vivo* compared to HAdV-C5. We propose that the enhanced anti-tumor effects are at least in part attributable to the use of different entry receptors by these viruses, although additional aspects of virus biology should not be disregarded. Regardless, our work demonstrates that GoraVir exhibits unique oncolytic properties and seems a promising candidate for the treatment of PDAC through targeting of tumor cells and tumor-adjacent stroma.

Data availability

The data that support the findings of this study are available from the corresponding author upon reasonable request.

Author contributions: S.T.F.B conceived the outline of the project. S.T.F.B., T.J.H., and C.G. designed the experiments. S.T.F.B., T.J.H., C.G., P.K., and V.K. conducted the experiments. S.T.F.B. acquired and analyzed the data. S.T.F.B., T.J.H., and R.C.H. wrote the article. N.v.M. and R.C.H. interpreted the data and critically revised the article. All authors read and approved the final article.

Acknowledgements: We thank the Flow cytometry Core Facility (FCF) of Leiden University Medical Center (LUMC) in Leiden, the Netherlands, for technical support. We thank Martijn Rabelink and Evelien Jonge-Muller for their technical assistance. This research was funded, in part, by the Foundation ‘‘Overleven met Alvleesklierkanker’’ Utrecht, Netherlands (OAK_LUMC-2017-2).

Conflict of interests: S.T.F.B., V.K., and R.C.H. are named inventors of patents pertaining to the use of human- and non-human primate-derived adenoviruses as viral vectors or as oncolytic agents. R.C.H. received and receives research funds from Janssen Vaccines & Prevention B.V. (Leiden, Netherlands) for projects on adenoviruses. The funders had no role in the design of the study; in the collection, analyses, or interpretation of data; in the writing of the article; or in the decision to publish the results. The authors declare no other conflict of interests and have no other relevant affiliation or financial involvement with any organization or entity with a financial interest in or financial conflict with the subject matter or materials discussed in the article, apart from those disclosed.

LITERATURE

[1] Sarantis P, Koustas E, Papadimitropoulou A, Papavassiliou AG, & Karamouzis MV (2020) Pancreatic ductal adenocarcinoma: Treatment hurdles, tumor microenvironment and immunotherapy. World J Gastrointest Oncol 12, doi: 10.4251/wjgo.v12.i2.173

[2] Timmer FEF, Geboers B, Nieuwenhuizen S, Dijkstra M, Schouten EAC, Puijk RS, de Vries JJJ, van den Tol MP, Bruynzeel AME, Streppel MM, Wilmink JW, van der Vliet HJ, Meijerink MR, Scheffer HJ & de Gruijl TD (2021) Pancreatic cancer and immunotherapy: A clinical overview. Cancers 13, doi: 10.3390/cancers13164138

[3] Gujar S, Pol JG & Kroemer G (2018) Heating it up: Oncolytic viruses make tumors “hot” and suitable for checkpoint blockade immunotherapies. OncoImmunology 7, doi: 10.1080/2162402X.2018.1442169

[4] Macedo N, Miller DM, Haq R & Kaufman HL (2020) Clinical landscape of oncolytic virus research in 2020. J Immunother Cancer 8, doi: 10.1136/jitc-2020-001486

[5] Taipale K, Liikanen I, Koski A, Heiskanen R, Kanerva A, Hemminki O, Oksanen M, Grönberg-Vähä-Koskela S, Hemminki K, Joensuu T & Hemminki Akseli (2016) Predictive and prognostic clinical variables in cancer patients treated with adenoviral oncolytic immunotherapy. Molecular Therapy 24, doi: 10.1038/mt.2016.67

[6] Vogels R, Zuijdgeest D, van Rijnsoever R, Hartkoorn E, Damen I, de Bethune MP, Kostense S, Penders G, Helmus N, Koudstaal W, Cecchini M, Wetterwald A, Sprangers M, Lemckert A, Ophorst O, Koel B, van Meerendonk M, Quax P, Panitti L, Grimbergen J, Bout A, Goudsmit J & Havenga M (2003) Replication-deficient human adenovirus type 35 vectors for gene transfer and vaccination: Efficient human cell infection and bypass of preexisting adenovirus immunity. J Virol 77, doi: 10.1128/jvi.77.15.8263-8271.2003

[7] Tomita K, Sakurai F, Tachibana M & Mizuguchi H (2012) Correlation between adenovirus-neutralizing antibody titer and adenovirus vector-mediated transduction efficiency following intratumoral injection. Anticancer Res 32, 1145-1152

[8] Bots STF & Hoeben RC (2020) Non-human primate-derived adenoviruses for future use as oncolytic agents? Int J Mol Sci 21, doi: 10.3390/ijms21144821

[9] Bots STF, Kemp V, Cramer SJ, van den Wollenberg DJM, Hornsveld M, Lamfers MLM, van der Pluijm G & Hoeben RC (2022) Nonhuman primate adenoviruses of the Human Adenovirus B species are potent and broadly acting oncolytic vector candidates. Hum Gene Ther 33, doi: 10.1089/hum.2021.216

[10] Giacinti C & Giordano A (2006) RB and cell cycle progression. Oncogene 25, doi: 10.1038/sj.onc.1209615

[11] Suzuki K, Fueyo J, Krasnykh V, Reynolds PN, Curiel DT & Alemany R (2001) A conditionally replicative adenovirus with enhanced infectivity shows improved oncolytic potency. Clin Cancer Res 7, 120–126

[12] Yu Y, Yang G, Huang H, Fu Z, Cao Z, Zheng L, You L & Zhang T (2021) Preclinical models of pancreatic ductal adenocarcinoma: Challenges and opportunities in the era of precision medicine. J Exp Clin Cancer Res 40, doi: 10.1186/s13046-020-01787-5

[13] Narayanan S, Vicent S & Ponz-Sarvisé M (2021) PDAC as an immune evasive disease: Can 3D model systems aid to tackle this clinical Pproblem? Front Cell Dev Biol 9, doi: 10.3389/fcell.2021.787249

[14] Harryvan TJ, Hawinkels LJAC, mini-tumor workgroup, Östman A, ten Dijke P, Strell C & Hornsveld M (2022) A novel pancreatic cancer mini-tumor model to study desmoplasia and myofibroblastic cancer-associated fibroblast differentiation. Appl Geochem 1, doi: 10.1016/j.gastha.2022.04.019

[15] F Froeling FEM, Mirza TA, Feakins RM, Seedhar A, Elia G, Hart IR & Kocher HM (2009) Organotypic culture model of pancreatic cancer demonstrates that stromal cells modulate E-cadherin, β-catenin, and ezrin expression in tumor cells. Am J Pathol 175, doi: 10.2353/ajpath.2009.090131

[16] Harryvan TJ, Golo M, Dam N, Schoonderwoerd MJA, Farshadi EA, Hornsveld M, Hoeben RC, Hawinkels LJAC & Kemp V (2022) Gastrointestinal cancer-associated fibroblasts expressing Junctional Adhesion Molecule-A are amenable to infection by oncolytic reovirus. Cancer Gene Ther, doi: 10.1038/s41417-022-00507-9

[17] Sanjana NE, Shalem O & Zhang F (2014) Improved vectors and genome-wide libraries for CRISPR screening. Nat Methods 11, doi: 10.1038/nmeth.3047

[18] Dull T, Zufferey R, Kelly M, Mandel RJ, Nguyen M, Trono D & Naldin L (1998) A third-generation lentivirus vector with a conditional packaging system. ASM 72, 8463–8471

[19] Monteran L & Erez N (2019) The dark side of fibroblasts: Cancer-associated fibroblasts as mediators of immunosuppression in the tumor microenvironment. Front Immunol 10, doi: 10.3389/fimmu.2019.01835

[20] Liu T, Han C, Wang S, Fang P, Ma Z, Xu L & Yin R (2019) Cancer-associated fibroblasts: An emerging target of anti-cancer immunotherapy. J Hematol Oncol 12, doi: 10.1186/s13045-019-0770-1

[21] Geng X, Chen H, hao L, Hu J, Yang W, Li G, Cheng C, Zhao Z, Zhang T, Li L & Sun B (2021) Cancer-associated fibroblast (CAF) heterogeneity and targeting therapy of CAFs in pancreatic cancer. Front in Cell Dev Biol 9, doi: 10.3389/fcell.2021.655152

[22] Yakavets I, Francois A, Benoit A, Merlin JL, Bezdetnaya L & Vogin G (2020) Advanced co-culture 3D breast cancer model for investigation of fibrosis induced by external stimuli: Optimization study. Sci Rep 10, doi: 10.1038/s41598-020-78087-7

[23] Nemerow GR, Pachea L, Reddy V & Stewart PL (2009) Insights into adenovirus host cell interactions from structural studies. Virology 38423, doi: 10.1016/j.virol.2008.10.016

[24] McDonald D, Stockwin L, Matzow T, Blair Zajdel ME & Blair GE (1993) Coxsackie and adenovirus receptor (CAR)-dependent and major histocompatibility complex (MHC) class I-independent uptake of recombinant adenoviruses into human tumour cells. Gene Ther 6, doi: 10.1038/sj.gt.3301006

[25] Arnberg N (2009) Adenovirus receptors: Implications for tropism, treatment and targeting. Rev Med Virol 19, doi: 10.1002/rmv

[26] Magnusson MK, Hong SS, Boulanger P & Lindholm L (2001) Genetic retargeting of adenovirus: Novel strategy employing "deknobbing" of the fiber. J Virol 75, doi: 10.1128/jvi.75.16.7280-7289.2001

[27] You Z, Fischer DC, Tong X, Hasenburg A, Aguilar-Cordova E & Kieback DG (2001) Coxsackievirus-adenovirus receptor expression in ovarian cancer cell lines is associated with increased adenovirus transduction efficiency and transgene expression. Cancer Gene Ther 8, doi: 10.1038/sj.cgt.7700284

[28] Mizuguchi H & Hayakawa T (2002) Adenovirus vectors containing chimeric type 5 and type 35 fiber proteins exhibit altered and expanded tropism and increase the size limit of foreign genes. Gene 285, doi: 10.1016/S0378-1119(02)00410-9

[29] Ni S, Gaggar A, Di Paolo N, Li ZY, Liu Y, Strauss R, Sova P, Morihara J, Feng Q, Kiviat N, Toure P, Sow PS & Lieber A (2006) Evaluation of adenovirus vectors containing serotype 35 fibers for tumor targeting. Cancer Gene Ther 13, doi: 10.1038/sj.cgt.7700981

[30] Gaggar A, Shayakhmetov DM & Lieber A (2003) CD46 is a cellular receptor for group B adenoviruses. Nat Med 9, doi: 10.1038/nm952

[31] Tatsis N, Blejer A, Lasaro MO, Hensley SE, Cun A, Tesema L, Li Y, Gao G, Xiang ZQ, Zhou D, Wilson JM & Ertl HCJ (2007) A CD46-binding chimpanzee adenovirus vector as a vaccine carrier. Mol Ther 15, doi: 10.1038/sj.mt.6300078

[32] Hensen LCM, Hoeben RC & Bots STF (2020) Adenovirus receptor expression in cancer and its multifaceted role in oncolytic adenovirus therapy. Int J Mol Sci 21, doi:10.3390/ijms21186828

[33] Wang H, Li Z, Liu Y, Persson J, Beyer I, Möller T, Koyuncu D, Drescher MR, Strauss R, Zhang X, Wahl III JK, Urban N, Drescher C, Hemminki A, Fender P & Lieber A (2011) Desmoglein 2 is a receptor for adenovirus serotypes 3, 7, 11 and 14. Nat Med 17, doi: 10.1038/nm.2270

[34] von Seggern DJ, Huang S, Fleck SK, Stevenson SC & Nemerow GR (2000) Adenovirus vector pseudotyping in fiber-expressing cell lines: Improved transduction of Epstein-Barr virus-transformed B cells. ASM 74, 354-362

[35] Fueyo J, Gomez-Manzano C, Alemany R, Lee PSY, McDonnell TJ, Mitlianga P, Shi Y, Levin VA, Yung WKA & Kyritsis AP (2000) A mutant oncolytic adenovirus targeting the Rb pathway produces anti-glioma effect in vivo. Oncogene 19, doi: 10.1038/sj.onc.1203251

[36] Hassan F, Lossie SL, Kasik EP, Channon AM, Ni S & Kennedy MA (2018) A mouse model study of toxicity and biodistribution of a replication defective adenovirus serotype 5 virus with its

genome engineered to contain a decoy hyper binding site to sequester and suppress oncogenic HMGA1 as a new cancer treatment therapy. PLoS One 13, doi: 10.1371/journal.pone.0192882

[37] Wang X, Zhong L & Zhao Y (2021) Oncolytic adenovirus: A tool for reversing the tumor microenvironment and promoting cancer treatment. Oncol Rep 45, doi: 10.3892/OR.2021.8000

[38] Everts A, Bergeman M, McFadden MG & Kemp V (2020) Simultaneous tumor and stroma targeting by oncolytic viruses. Biomedicines 8, doi: 10.3390/biomedicines8110474

[39] Li M, Li G, Kiyokawa J, Tirmizi Z, Richardson LG, Ning J, Das S, Martuza RL, Stemmer-Rachamimov A, Rabkin SD & Wakimoto H (2020) Characterization and oncolytic virus targeting of FAP-expressing tumor-associated pericytes in glioblastoma. Acta Neuropathol Commun 8, doi: 10.1186/s40478-020-01096-0

[40] de Sostoa J, Fajardo CA, Moreno R, Ramos MD, Farrera-Sal M & Alemany R (2019) Targeting the tumor stroma with an oncolytic adenovirus secreting a fibroblast activation protein-targeted bispecific T-cell engager. J Immunother Cancer 7, doi: 10.1186/s40425-019-0505-4

[41] Elvington M, Liszewski MK & Atkinson JP (2020) CD46 and oncologic interactions: Friendly fire against cancer. Antibodies 9, doi: 10.3390/antib9040059

[42] Hulin-Curtis SL, Uusi-Kerttula H, Jones R, Hanna L, Chester JD & Parker AL (2016) Evaluation of CD46 re-targeted adenoviral vectors for clinical ovarian cancer intraperitoneal therapy. Cancer Gene Ther 23, doi: 10.1038/cgt.2016.22

[43] Do M, To PK, Cho Y, Kwon S, Hwang EC, Choi C, Cho S, Lee S, Hemmi S & Jung C (2018) Targeting CD46 enhances anti-tumoral activity of adenovirus type 5 for bladder cancer. Int J Mol Sci 19, doi: 10.3390/ijms19092694

[44] Hess C & Kemper C (2016) Complement-mediated regulation of metabolism and basic cellular processes. Immunity 45, doi: 10.1016/j.immuni.2016.08.003

[45] José A, Sobrevals L, Camacho-Sánchez JM, Huch M, Andreu N, Ayuso E, Navarro P, Alemany R & Fillat C (2013) Intraductal delivery of adenoviruses targets pancreatic tumors in transgenic Ela-myc mice and orthotopic xenografts. Oncotarget 4, doi: 10.18632/oncotarget.795

[46] Yu YA, Galanis C, Woo Y, Chen N, Zhang Q, Fong Y & Szalay AA (2009) Regression of human pancreatic tumor xenografts in mice after a single systemic injection of recombinant vaccinia virus GLV-1h68. Mol Cancer Ther 8, doi: 10.1158/1535-7163.MCT-08-0533

[47] Bergelson JM, Krithivas A, Celi L, Droguett G, Horwitz MS, Wickham T, Crowell RL & Finberg RW (1998) The murine CAR homolog is a receptor for coxsackie B viruses and adenoviruses. ASM 72, 415-419

[48] Murali VK, Ornelles DA, Gooding LR, Wilms HT, Huang W, Tollefson AE, Wold WSM & Garnett-Benson C (2014) Adenovirus death protein (ADP) is required for lytic infection of human lymphocytes. J Virol 88, doi: 10.1128/jvi.01675-13

[49] Chaurasiya S, Fong Y & Warner SG (2021) Oncolytic virotherapy for cancer: Clinical experience. Biomedicines 9, doi: 10.3390/biomedicines9040419

[50] Martin NT, Roy DG, Workenhe ST, van den Wollenberg DJM, Hoeben RC, Mossman KL, Bell JC & Bourgeois-Daigneault MC (2018) Pre-surgical neoadjuvant oncolytic virotherapy confers protection against rechallenge in a murine model of breast cancer. Sci Rep 9, doi: 10.1038/s41598-018-38385-7

FIGURE LEGENDS

Figure 1. Infection of pancreatic cancer cells and cancer-associated fibroblasts with GoraVir. A) Pancreatic cancer cell lines BxPC-3, PATU-T and MIA PaCa-2, as well as the patient-derived pancreatic cancer cell line FNA005, and B) the pancreatic stellate cell line PS-1 were infected with GoraVir or HAdV-C5 at multiplicity of infection (MOI) 0.1 or MOI 10 and cell viability was measured by WST assay at day 6 post infection. Mean is depicted relative to uninfected cells of n=2 (FNA005) or n=3 biological replicates each performed in triplicate; C) Patient-derived primary fibroblasts isolated from pancreatic cancer tissues were infected with GoraVir MOI 10 and cell viability was measured by WST assay at day 5 post infection. Mean is depicted relative to uninfected cells of a representative figure of n=2 biological replicates each performed in triplicate. The dashed line denotes 50% reduction in cell viability.

Figure 2. Lytic potential of GoraVir and HAdV-C5 in PDAC spheroid cultures. A) Light microscopy pictures of spheroid monocultures of the pancreatic cancer cell line BxPC-3 and the patient-derived pancreatic cancer cell line FNA005, and hematoxylin and eosin (HE) staining of co-cultures of these cells with the stellate cell line PS-1. Scale bar represents 200 µm (light microscopy) and 500 µm (HE) size; B) Spheroid monocultures of BxPC-3 or C) FNA005 cells were infected with GoraVir or HAdV-C5 at different multiplicity of infection (MOI) and cell viability was determined at 5 days post infection. Means are depicted relative to uninfected cells, and each symbol represents an individual spheroid. Statistical analyses were performed using multiple unpaired t tests and the Holm-Šídák correction. Significant differences are indicated by asterisks, with p values <0.01 shown as **, and < 0.001 shown as ***; D) Immunohistochemistry (IHC) staining of adenovirus hexon protein (brown) in BxPC-3/PS-1 co-culture spheroids infected with virus at MOI 10 at 3 and 5 days post infection. Black arrows indicate signs of cytopathic effect (CPE). Illustrated are representative spheroids of n=5. Scale bar represents 500 µm size.

Figure 3. Infection of MIA PaCa-2 CD46 knockout cells with GoraVir and HAdV-C5. A) Cell surface protein expression of CAR, CD46, and DSG-2 on unstained (-), wildtype (WT), empty vector (EV) control, or CD46 knock out (KO) MIA PaCa-2 cells; B) WT, EV, and KO MIA PaCa-2 cells were infected with GoraVir or HAdV-C5 at multiplicity of infection (MOI) 10 for 48 hours after which hexon protein expression was measured by flow cytometry. Depicted are representative figures of n=3 biological replicates; C) Percentage of hexon positive cells relative to WT-infected cells. Depicted are means of n=3 biological replicates; D) WT, EV, and KO MIA PaCa-2 cells were infected with GoraVir or E) HAdV-C5 at different MOI and cell viability was measured by WST assay at 6 days post infection. Depicted are mean ± SEM of n=3 independent experiments each performed in triplicate.

Figure 4. Single-dose intratumoral injection of GoraVir or HAdV-C5Δ24E3 in a BxPC-3 xenograft model. A) NSG mice were subcutaneously injected with 5 x 10^6 BxPC-3 cells and upon the presence of palpable tumors, PBS or 1 x 10^8 plaque forming units of GoraVir or HAdV-C5Δ24E3 was injected intratumorally. Depicted are the individual tumor growth curves of PBS control group, GoraVir, or HAdV-C5Δ24E3-treated mice (n=5 per group). The dashed line denotes the start of the treatment; B) Mean tumor volume and C) tumor weight on day 10 post injection for PBS, GoraVir, and HAdV-C5Δ24E3-treated mice (n=5 per group); D) Mean Ad genome copies in tumor tissue, serum, liver, and spleen on day 10 post injection GoraVir and HAdV-C5Δ24E3-treated mice (n=5 per group). Statistical analyses were

performed using one-way ANOVA and the Tukey correction. Significant differences are indicated by asterisks, with p values <0.05 shown as *, <0.01 shown as **, and < 0.001 shown as ***.

SUPPORTING INFORMATION

Supplementary Table S1. EC50 values for GoraVir and HAdV-C5 in pancreatic cancer cells and cancer-associated fibroblasts.

Supplementary Figure S1. Infection of A549 CD46 knockout cells with GoraVir and HAdV-C5.

Supplementary Figure S2. mRNA expression of CAR and CD46 in patient-derived primary fibroblasts.

Supplementary Figure S3. Mice body weight upon treatment with PBS, GoraVir, or HAdV-C5Δ24E3.

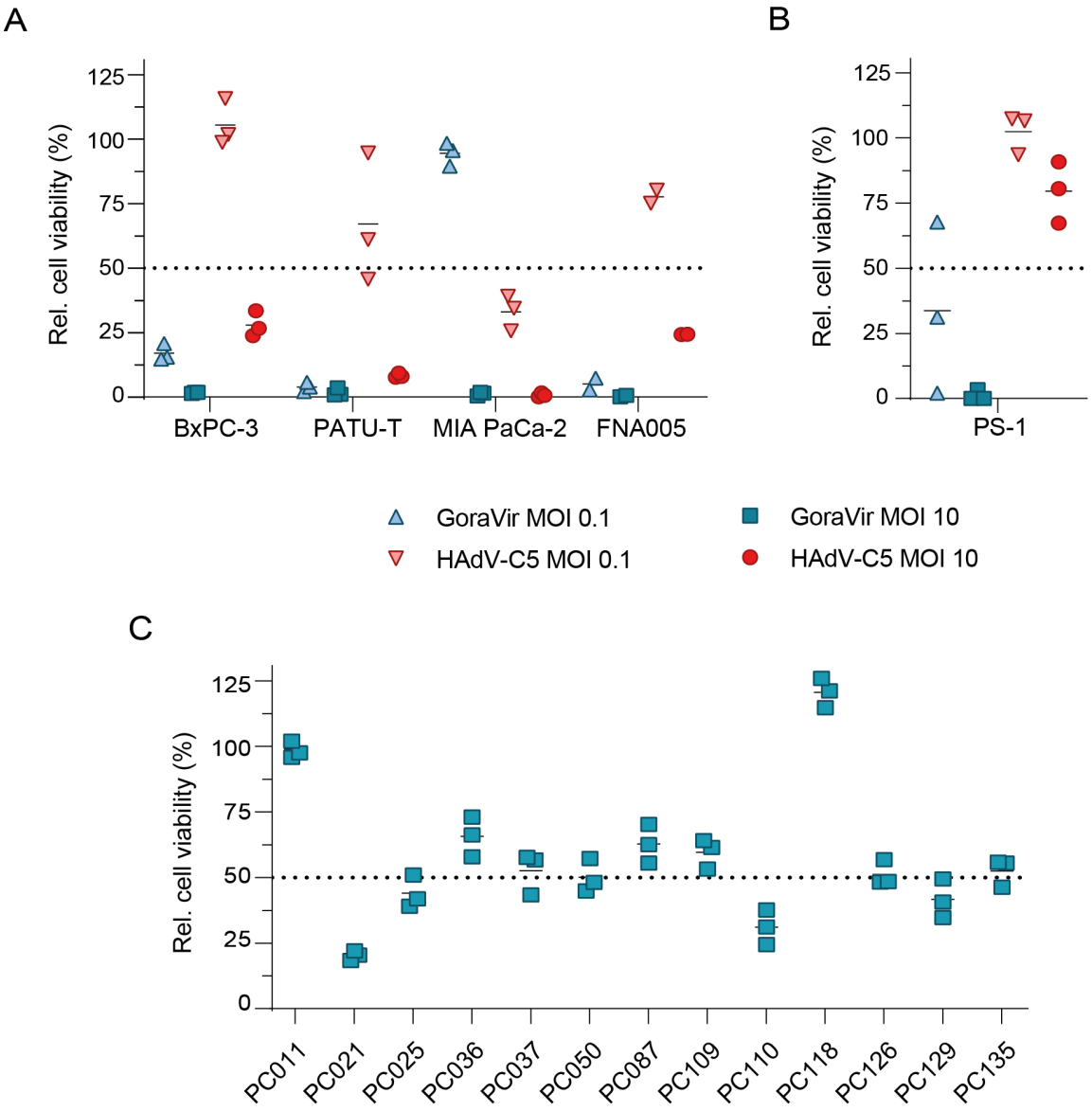

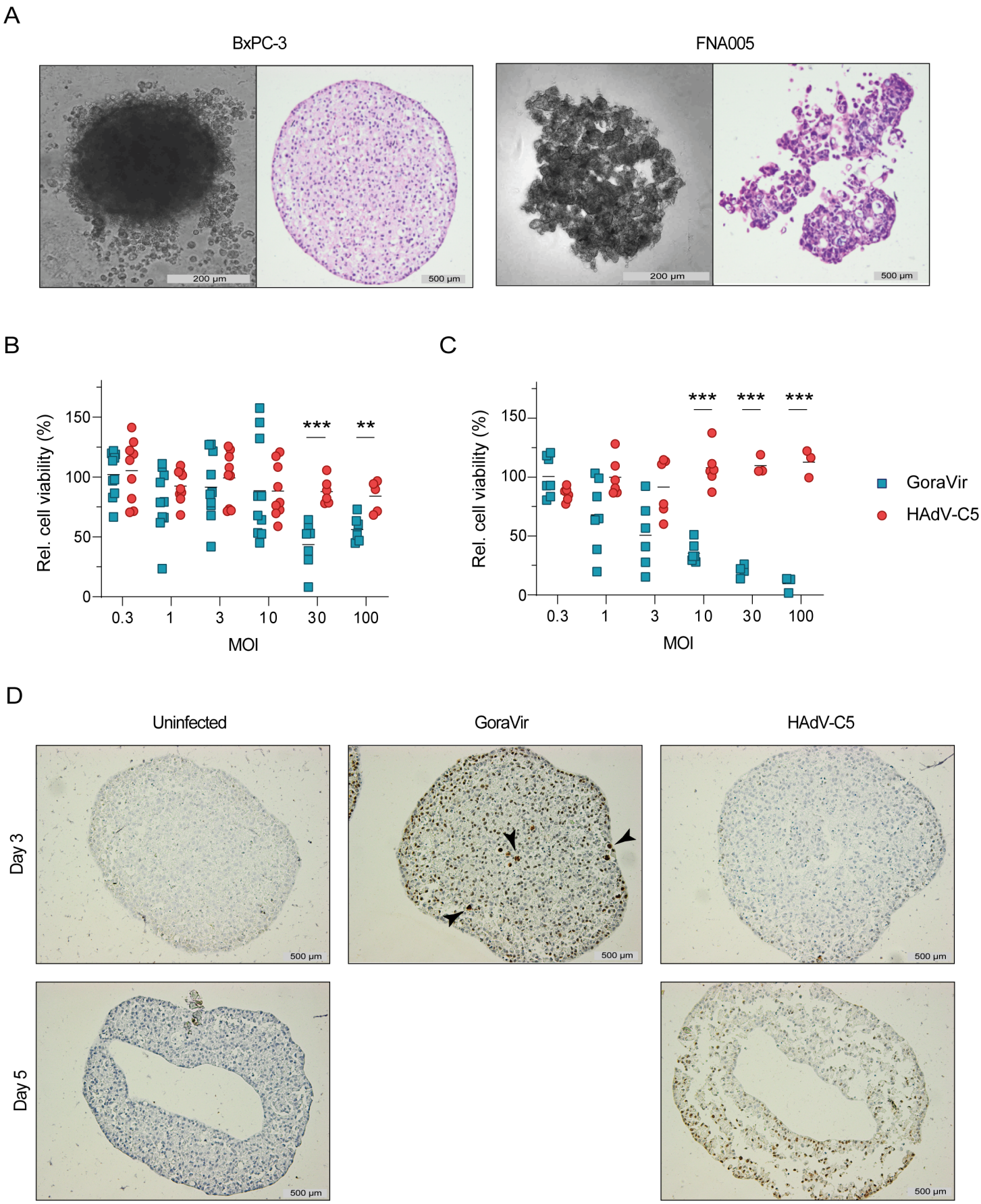

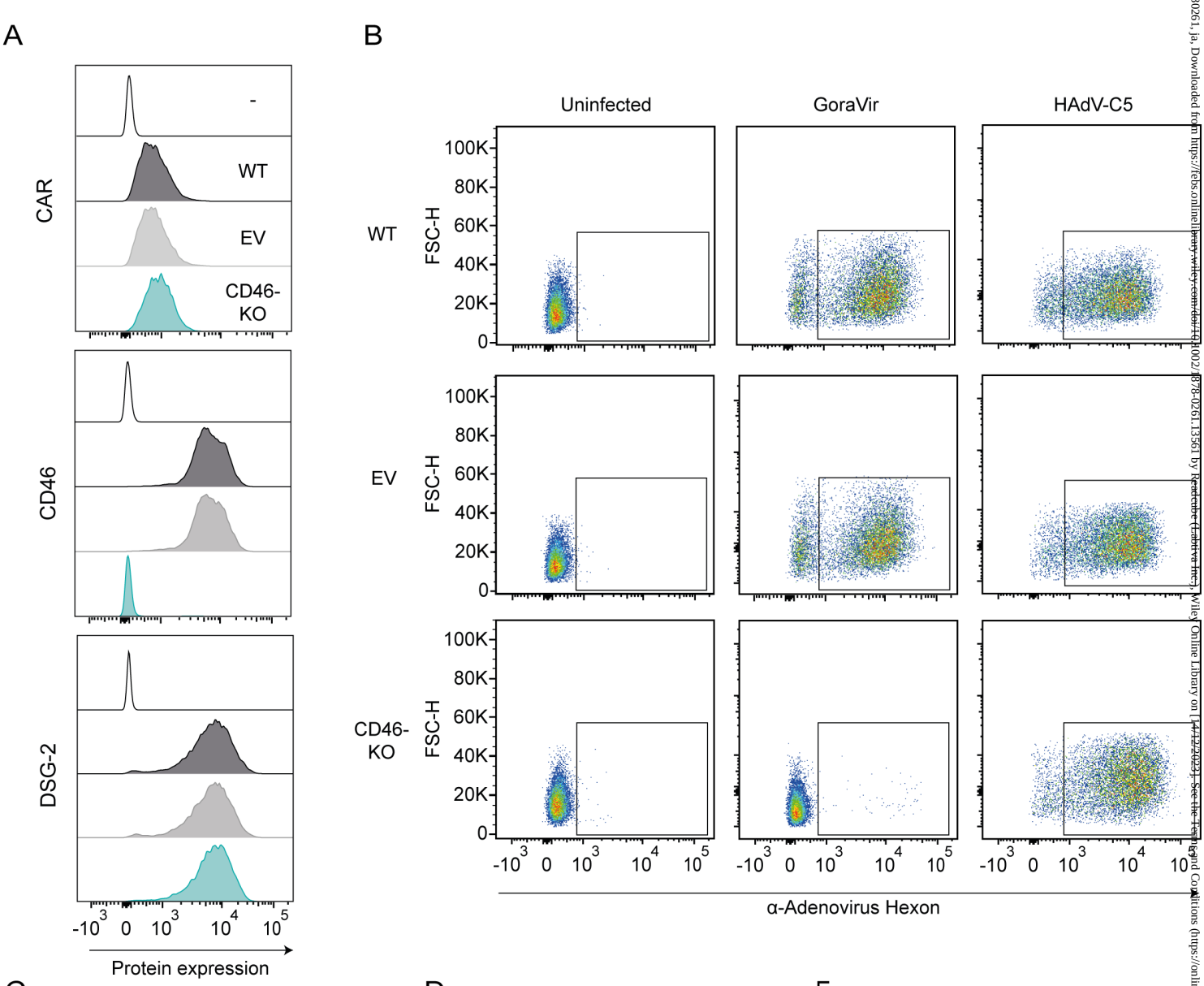

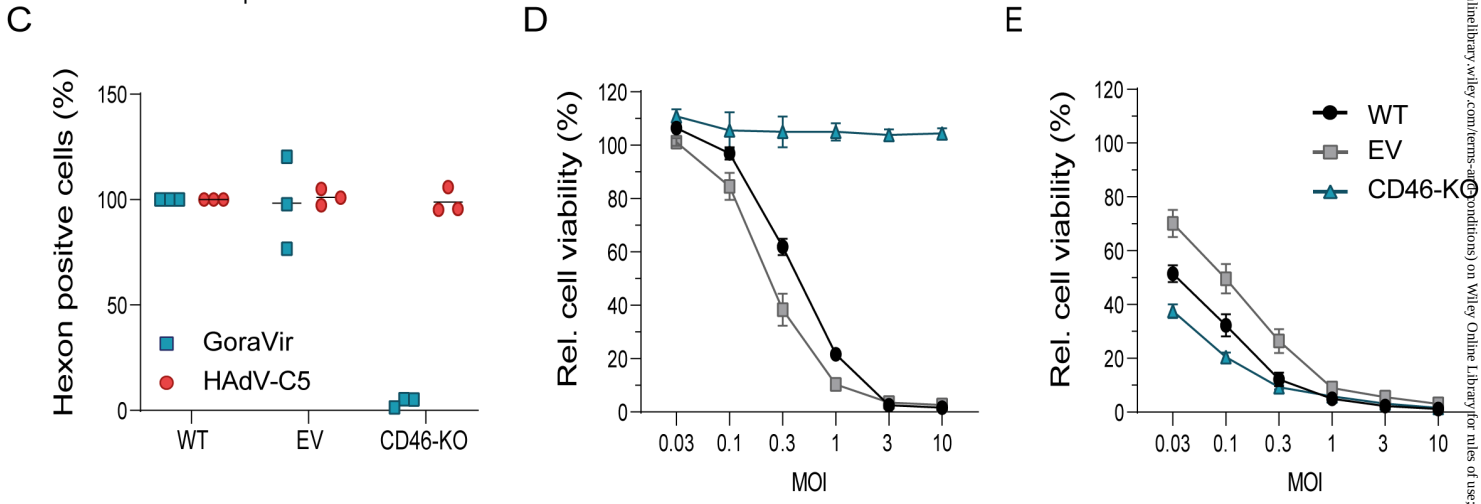

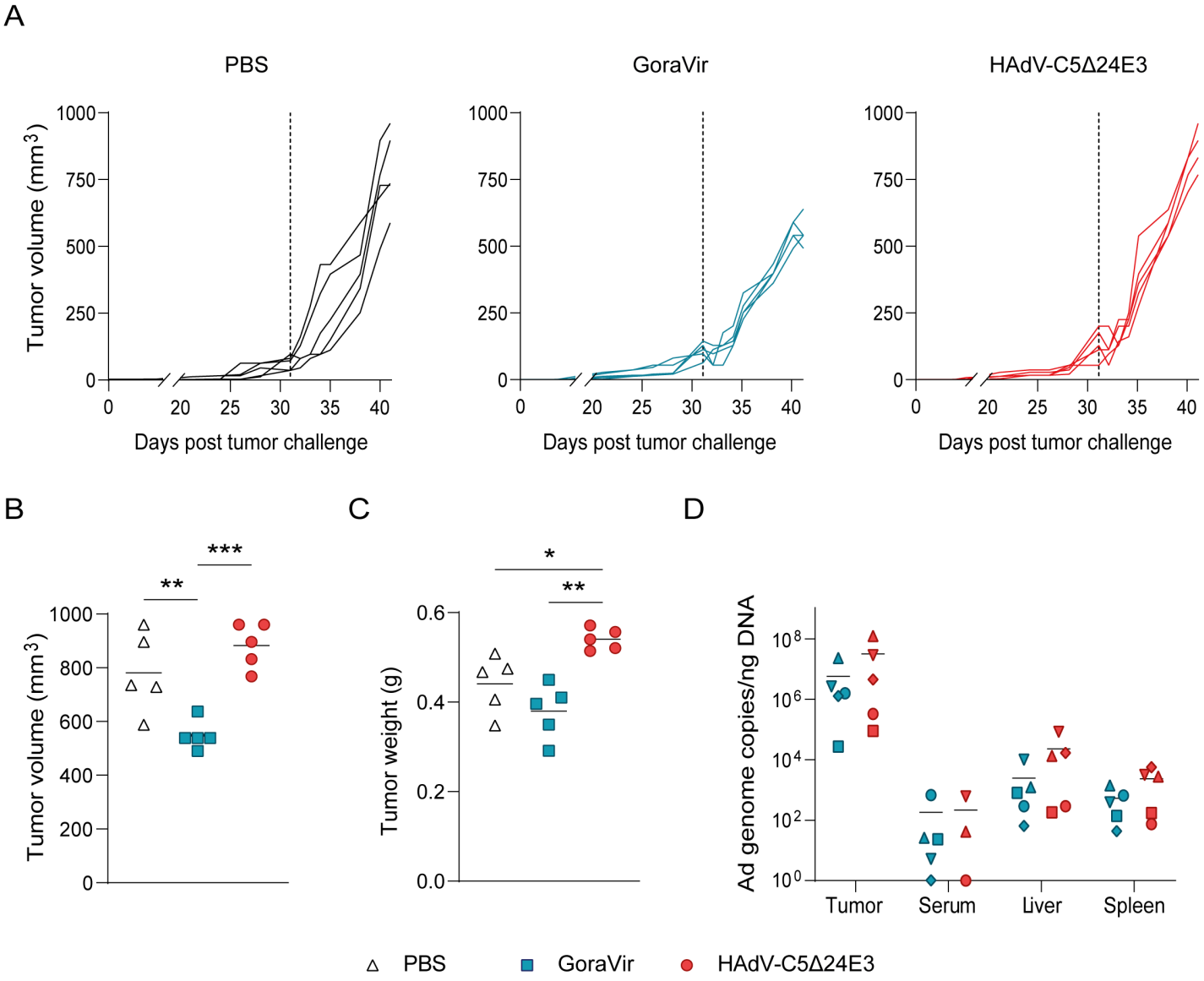

First of all we would like to thank the reviewers for their insightful comments to our manuscript. We respond to these comments below.

Reviewer: 1

Comments to the Author

my concerns have all been well addressed

Thank you for your feedback.

Reviewer: 2

Comments to the Author

I am sorry to see that my comment from last round was not addressed at all:

There is conflict of the cell lines, and DSG2 data:

"Figure 3, the DSG-2 expression level conflicts with previously published data (PMID: 22086234, 36016457 and 36016457). In both studies, different than the current manuscript with almost 100% detection, low DSG-2 level were detected. The Authors need to address this, by experiment repeats, and with different anti-DSG-2 antibodies."

The answer to reviewer's commet in the first round:

"We solved the discrepancy, but in a somewhat unexpected manner. During our control experiments in which we used a different source of DSG -2 antisera, we were informed that there has been a mix -up in our department's cell collection. STR analysis of the vials labeled MIA PaCa-2 cells contain, in fact, PANC-1 cells. Ampoules made at the onset of our studies also contain PANC-1 cells. Therefore we replaced the name of MIA PaCa-2 throughout our manuscript by PANC-1."

In the second round:

"Based on our initial findings, the administrators of our cell bank have conducted STR -analys es o n all cell lines currently available in our database as well as the specific cell lines used in this manuscript. After thorough analysis, we validate d the authenticity of the BxPC -3 and MIA PaCa -2 cell line s used in this manuscript but identified the HPAF -II cell line as PATU - T (RRID:CVCL_1847). We are grateful to the cell line bank administrators for recognizing the problem and helping us trace the correct identities of the cell lines used. This incident has most definitely raised the awareness on the cell -line identity issue in our institute as well as the importance of frequent cell line validation. We have replaced the name of HPAF -II throughout the manuscript with PATU -T. This incident has no consequences for any of the conclusions that could be drawn from the data presented in this manuscript"

Due to a mix-up during cell line retrieval from our cell line collection, we incorrectly assumed that all our MIA PaCa-2 cells were PANC-I cells. That assumption was proven incorrect, and all experiments that we show in the manuscript are done with STR-validated Mia PaCa-2 cells (appendix fig 1).

This leaves the issue of the DSG2 expression on the MIA PaCa-2 cells described as DSG2-negative in literature. We repeated the flowcytometric analyses on DSG2 expression in STR-validated MIA PaCa-2 cells and found our cells to be DSG2-positive using the CSTEM28 antiserum directed against DSG2 from eBioscience (appendix fig 2). STR-validated MIA PaCa-2 cells from Heidelberg, Germany, exhibited only a small fraction of DSG2-positive cells using the same antiserum.

To further validate DSG2 expression, we generated cDNA from our MIA PaCa-2 cells for use in rt-PCR and obtained a clear PCR product (appendix fig 3). Sequence analysis of this 474 bp PCR fragment yielded a sequence that is fully identical to part of the published human DSG2 cDNA (Genbank accession number NM_001943). These data show without doubt that MIA PaCa-2 cells can express DSG2. Both in the PCR as well as in the flow cytometry analysis, the DSG2 levels detected in the MIA PaCa-2 cell line were very similar to HT29 cells, which we included as a positive control.

The varying expression levels in STR-confirmed MIA PaCa-2 cells from various sources may be due to differences in medium or serum composition, as was published before. Denning et al. (Exp. Cell Res. (1998)

239, 50–59) show that DSG2 expression is influenced by the calcium concentration in the medium of several normal, immortalized, and cancer cell lines. We assume that this may have affected the DSG2 levels in our MIA PaCa-2 cells and the MIA PaCa-2 cells from Germany.

We hope that this clarifies the matter. We apologize for the errors made and the confusion that this caused regarding the cell lines' identities. Please be assured that the names used in the current manuscript are correct and validated.

Appendices:

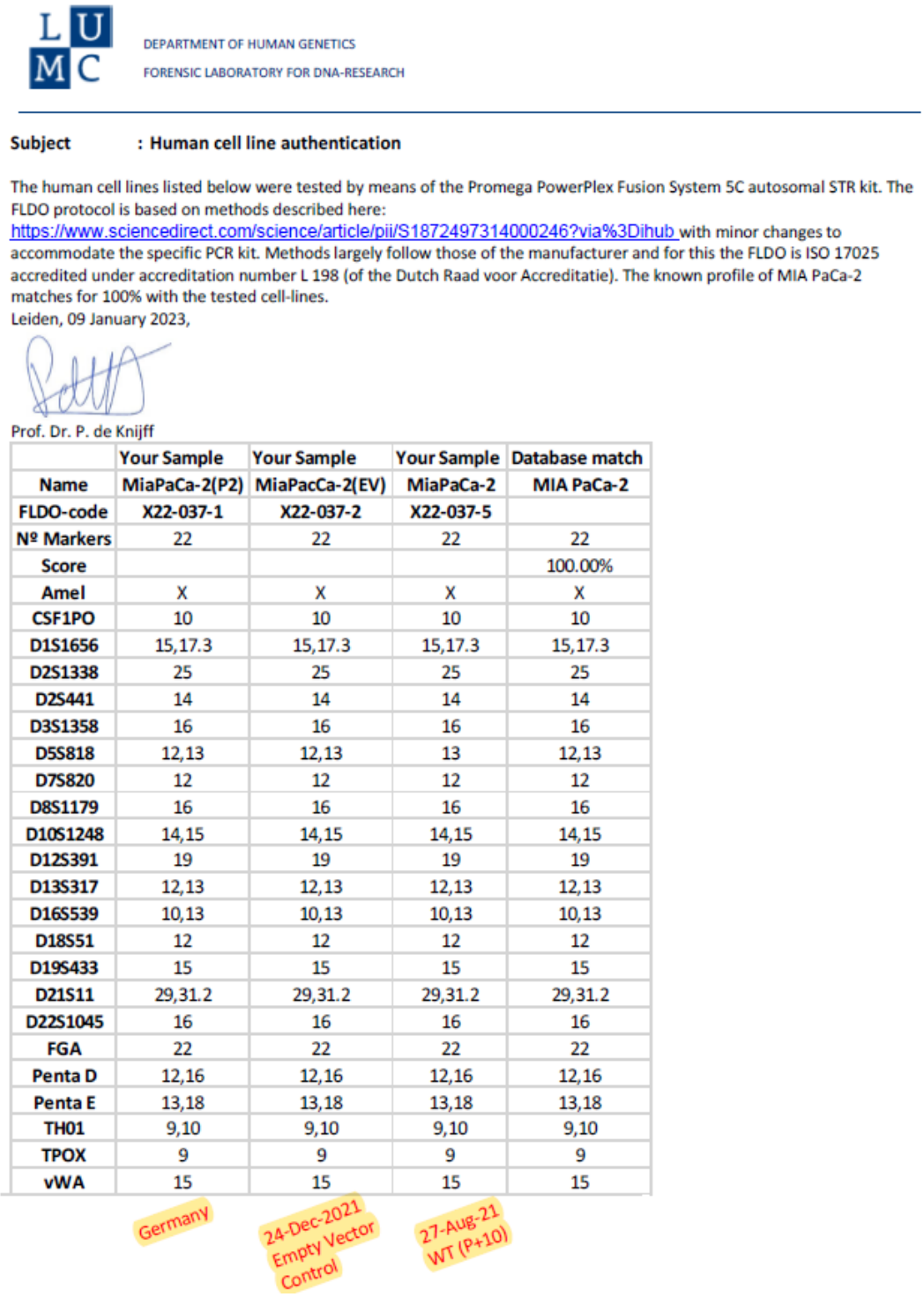

DEPARTMENT OF HUMAN GENETICS
FORENSIC LABORATORY FOR DNA-RESEARCH

Subject : Human cell line authentication

The human cell lines listed below were tested by means of the Promega PowerPlex Fusion System 5C autosomal STR kit. The FLDO protocol is based on methods described here: https://www.sciencedirect.com/science/article/pii/S1872497314000246?via%3Dihub with minor changes to accommodate the specific PCR kit. Methods largely follow those of the manufacturer and for this the FLDO is ISO 17025 accredited under accreditation number L 198 (of the Dutch Raad voor Accreditatie). The known profile of MIA PaCa-2 matches for 100% with the tested cell-lines.

Leiden, 09 January 2023,

Prof. Dr. P. de Knijff

	Your Sample	Your Sample	Your Sample	Database match
Name	MiaPaCa-2(P2)	MiaPacCa-2(EV)	MiaPaCa-2	MIA PaCa-2
FLDO-code	X22-037-1	X22-037-2	X22-037-5	
Nº Markers	22	22	22	22
Score				100.00%
Amel	X	X	X	X
CSF1PO	10	10	10	10
D1S1656	15,17.3	15,17.3	15,17.3	15,17.3
D2S1338	25	25	25	25
D2S441	14	14	14	14
D3S1358	16	16	16	16
D5S818	12,13	12,13	13	12,13
D7S820	12	12	12	12
D8S1179	16	16	16	16
D10S1248	14,15	14,15	14,15	14,15
D12S391	19	19	19	19
D13S317	12,13	12,13	12,13	12,13
D16S539	10,13	10,13	10,13	10,13
D18S51	12	12	12	12
D19S433	15	15	15	15
D21S11	29,31.2	29,31.2	29,31.2	29,31.2
D22S1045	16	16	16	16
FGA	22	22	22	22
Penta D	12,16	12,16	12,16	12,16
Penta E	13,18	13,18	13,18	13,18
TH01	9,10	9,10	9,10	9,10
TPOX	9	9	9	9
vWA	15	15	15	15

Germany
24-Dec-2021 Empty Vector Control
27-Aug-21 WT (P+10)

Fig 1 Results from STR-analysis of MIA PaCa-2 cells used in this manuscript. MIA PaCa-2 cells obtained from Heidelberg, Germany were included as a positive control.

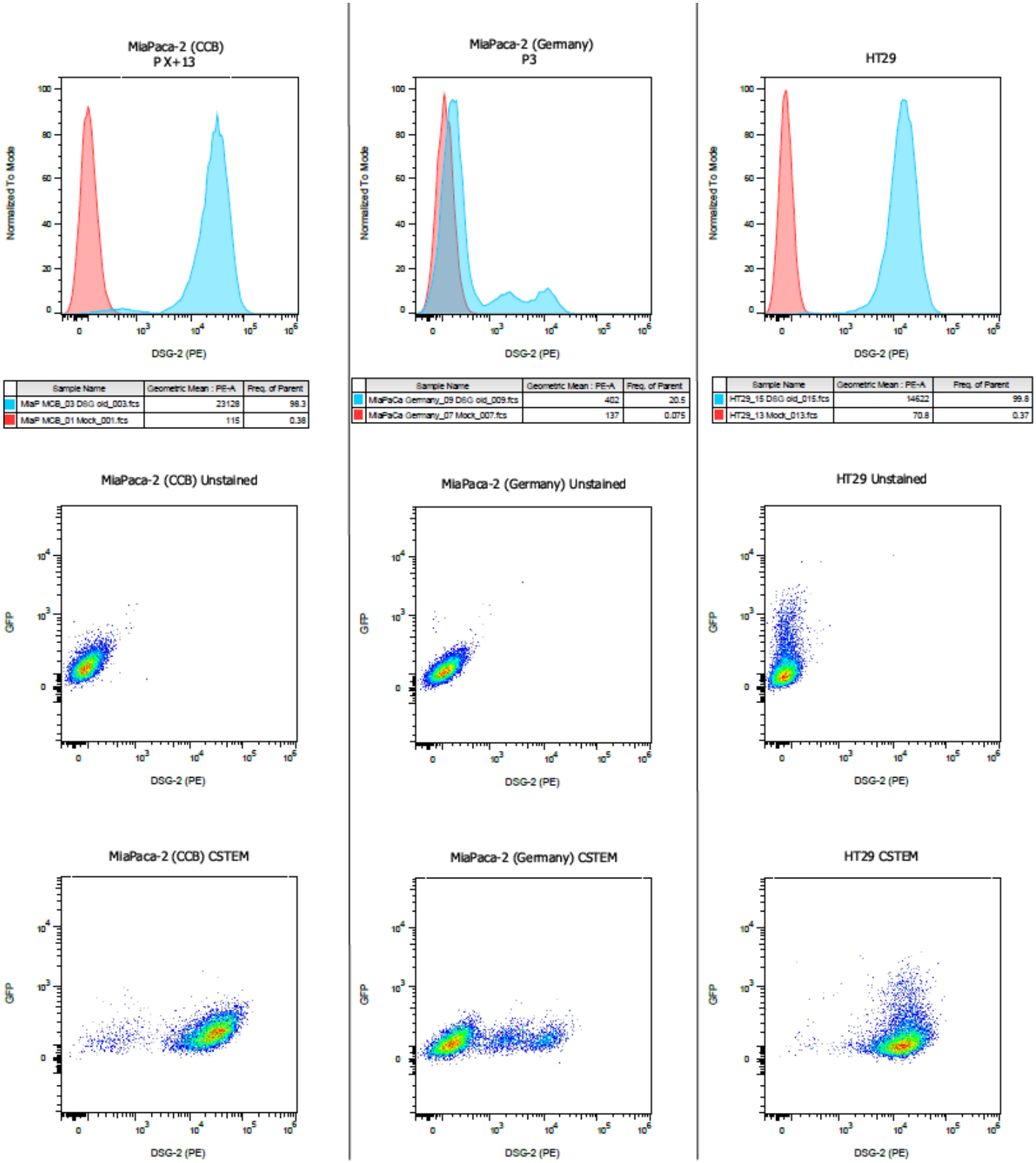

Fig 2 Protein expression of DSG2 from STR-validated MIA PaCa-2 cells using the CSTEM28 antiserum against DSG2. HT29 cells were included as a positive control.

hDSG-2_474PCR_For	gatagagcctgtgcagacaatctg	24-mer	Primer for PCR product [474 bp] - for sequencing cDNA Binds at: 1745 -> 1768
hDSG-2_474PCR_Rev	caaggatgcagcatctctatggtg	24-mer	Primer for PCR product [474 bp] - for sequencing cDNA Binds at: 2195 <- 2218

Fig 3A Primer sequences used for rtPCR analysis of DSG2 expression in MIA PaCa-2 cells.

5′- gataga gcctgtgcag acaatctgtc acgatgcaga gtatgtgaat gttactgcag
aggacctgga tggacaccca aacagtggcc ctttcagttt ctccgtcatt gacaaaccac
ctggcatggc agaaaaatgg aaaatagcac gccaagaaag taccagtgtg ctgctgcaac
aaagtgagaa aaagcttggg agaagtgaaa ttcagttcct gatttcagac aatcagggtt
ttagttgtcc tgaaaagcag gtccttacac tcacagtttg tgagtgtctg catggcagcg
gctgcaggga agcacagcat gactcctatg tgggcctggg acccgcagca attgcgctca
tgattttggc ctttctgctc ctgctattgg taccactttt actgctgatg tgccattgcg
gaaagggcgc caaaggcttt acccccatac ctggcaccat agagatgctg catccttg-3′

Fig 3B Nucleotide sequence of the DSG2 cDNA rtPCR fragment generated from RNA extracted from STR-validated MIA PaCa-2 cells. The sequence obtained is fully identical to a fragment of the nucleotide sequence of the human DSG2 cDNA (NM_001943), confirming that in these cells the MIA PaCa-2 express the DSG2 encoding gene.